THE JOURNAL OF PHYSICAL CHEMISTRY A LETTERS

2008, *112,* 11514–11518
Published on Web 10/23/2008

Monitoring Reaction Intermediates in the $FeCl_3$-Catalyzed Michael Reaction by Nuclear Inelastic Scattering

T. Asthalter,*,† S. Rajagopalan,† Th. Kauf,‡ V. Rabe,‡ and J. Christoffers§

Institut für Physikalische Chemie, Universität Stuttgart, Pfaffenwaldring 55, D-70569 Stuttgart, Germany, Institut für Organische Chemie, Universität Stuttgart, Pfaffenwaldring 55, D-70569 Stuttgart, Germany, and Institut für Reine and Angewandte Chemie, Carl-von-Ossietzky-Universität Oldenburg, Carl-von-Ossietzky-Strasse 9-11, D-26111 Oldenburg, Germany

Received: August 01, 2008; Revised Manuscript Received: September 23, 2008

We present a study of the metal-centered vibrations in the first step of the Fe(III)-catalyzed Michael reaction. Nuclear inelastic scattering of synchrotron radiation was carried out on a shock-frozen solution of $FeCl_3 \cdot 6H_2O$ in 2-oxocyclopentane ethylcarboxylate (CPEH), as well as on the solid reference compounds $FeCl_3 \cdot 6H_2O$, $[N(CH_3)_4][FeCl_4]$, and $Fe(acac)_3$. In addition to the vibrations of the $FeCl_4^-$ anion at 133 and 383 cm^{-1}, a multitude of modes associated with the complex $Fe(CPE)_2(H_2O)_2$ could be identified. Normal-mode analysis on different isomers of the simplified model complex $Fe(acac)_2(H_2O)_2$ as well as that of the full complex carrying two entire CPE ligands was carried out using density functional calculations. Comparison with experiment suggests that the facial bis(diketonato) isomer probably dominates in the reaction mixture. Thus, we have identified for the first time the isomeric structure of an iron-based intermediate of a homogeneous catalytic reaction using nuclear inelastic scattering.

1. Introduction

The Michael addition of β-dicarbonyl compounds to α-H acidic carbonyl compounds[1,2] is one of the most important C−C bond-forming reactions in organic chemistry. When carried out in the presence of Fe(III) salts (for a scheme, see Figure 1), conversion takes place under relatively mild conditions.[3] A mechanism for the underlying catalytic cycle was proposed and corroborated by kinetic studies and density functional (DFT) calculations (ref 4 and Figure 2). Combined studies using XAS, UV/vis, and Raman spectroscopy[5] revealed that the compound formed in the first reaction step (i.e., when $FeCl_3 \cdot 6H_2O$ or $Fe(ClO_4)_3 \cdot 9H_2O$ is dissolved in the Michael donor 2-oxocyclopentane ethyl carboxylate, CPEH) can be described as a bis(diketonato)−iron(III) unit containing the anion (CPE^-) and is probably coordinated with two water molecules. Information on the precise geometry and bonding strengths is now mandatory in order to proceed toward understanding the nature of the species undergoing further reaction. Moreover, in addition to the $FeCl_4^-$ anion, which acts as an iron sink and therefore decreases the efficiency of the reaction, the existence of other chloroferrate species, such as $Fe_2Cl_7^-$, is under debate.[6]

Investigations of bonding strengths are traditionally the domain of IR absorption (where data below 400 cm^{-1} can only be obtained with high experimental effort owing to detector sensitivity limits) or Raman scattering. Nuclear inelastic scattering of synchrotron radiation[7−9] (NIS, also named NRVS, nuclear resonance vibrational spectroscopy, in part of the literature)[11] is a new method that monitors selectively the bonding around a resonant or Mössbauer nucleus. It may thus give unique information about symmetry and bonding at the active center of metal catalysts and has been extensively used for the study of spin-crossover compounds (ref 10 and references therein), biocatalytically active centers,[11−14] and related model compounds.[15,16] Here, we describe the first application of NIS to the characterization of intermediates at a homogeneous metal−organic catalyst in situ.

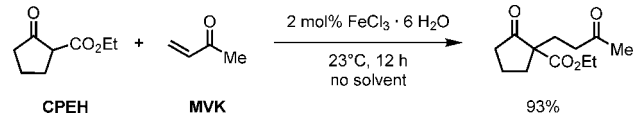

Figure 1. Reaction scheme of the Fe(III)-catalyzed Michael reaction.

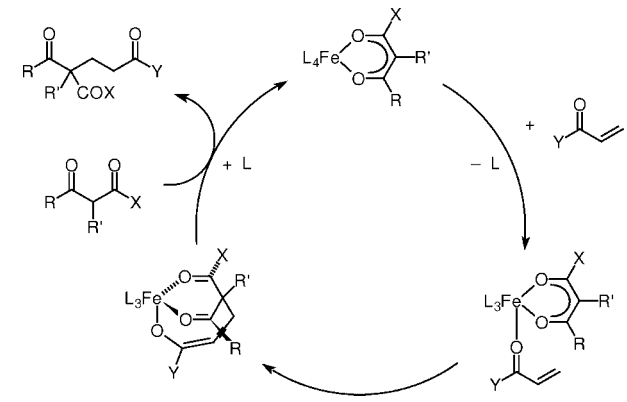

Figure 2. Proposed reaction mechanism of the Fe(III)-catalyzed Michael reaction.

* To whom correspondence should be addressed.
† Institut für Physikalische Chemie, Universität Stuttgart.
‡ Institut für Organische Chemie, Universität Stuttgart.
§ Carl-von-Ossietzky-Universität Oldenburg.

10.1021/jp806878x CCC: $40.75 © 2008 American Chemical Society

TABLE 1: Vibrational Wavenumbers of $FeCl_4^-$ for different DFT Functionals/Basis Sets/Methods, Together with Selected Experimental Data for Solid $[N(CH_3)_4][FeCl_4]$[a]

method	$\tilde{\nu}$ (E)/cm^{-1}	$\tilde{\nu}$ (T_2)/cm^{-1}	$\tilde{\nu}$ (A_1)/cm^{-1}	$\tilde{\nu}$ (T_2)/cm^{-1}	d (Fe−Cl)/Å	E/E_h
XRD[36]					2.171/2.178/2.191	
Raman[34]	114	136(vw)	330(vs)	378(vw)		
Raman	113	138(m)	338(vs)			
NIS		138(s)		383(vs)		
BP86/ext-pp/SDD	90	116	294.1	345	2.238	−1965.321
B3LYP/ext-pp/SDD	94	123	301	348	2.243	−1965.135
BP86/ext/all-e	97	127	313	359	2.230	−3105.063
B3LYP/ext/all-e	96	124	306	355	2.236	−3104.782
B3LYP/6-31G*/all-e	98	131	319	369	2.227	−3104.700
B3LYP[28]	99	133	320	370	2.230	−3104.701
UHF[28]	103	147	334	386	2.258	−3100.536

[a] The "ext" stands for the extended basis set by Ahlrichs described in the text for the all-electron calculations, and "ext-pp" are the extended basis set pseudopotential calculations (see text). $E_h = 27.2$ eV is the Hartree energy.

Spectra were taken on a frozen solution of $FeCl_3 \cdot 6H_2O$ in CPEH at 20 and 70 K (as described in refs 2 and 3, the entire reaction can be carried out on air, i.e. the solution is air-stable), as well as on the solid reference compounds $FeCl_3 \cdot 6H_2O$, $[N(CH_3)_4][FeCl_4]$, and $Fe(acac)_3$; see section 2. After description of the DFT calculations in section 3, the results are discussed in section 4.

2. Experimental Section

In NIS experiments with synchrotron radiation, the energy of the incoming photons is scanned around the nuclear resonance energy (14.4125 keV in the case of the most popular isotope ^{57}Fe) within a range of typical phonon energies. The detuned photons can excite the resonant nuclei by creation or annihilation of one or more phonons having the appropriate energy. After correcting for multiphonon excitations, one obtains the vibrational density of states (VDOS) of the resonant nucleus.

All samples were prepared from iron powder enriched to 95.3% in ^{57}Fe. $^{57}FeCl_3 \cdot 6H_2O$ was obtained by reacting the Fe powder with hydrochloric acid; $[N(CH_3)_4][FeCl_4]$ was subsequently obtained by reaction with $[N(CH_3)_4]Cl$.

The NIS experiments were carried out at the ID18 beamline of the European Synchrotron Radiation Facility using a high-resolution monochromator of the $+m$, $-n$, $-n$, $+m$ type[17,18] (inner crystals: Si (4 4 0); outer crystals: Si (10 6 4)), yielding an overall energy resolution of about 1.0 meV or 8 cm^{-1} for the measurements at 70 K and 1.2 meV or 9.6 cm^{-1} for the measurements at 20 K and ensuring high spectral flux.[19] The synchrotron was operated in hybrid mode with 24 × 8 bunches distributed over three-quarters of the ring and a single bunch in the center of the remaining quarter. The extraction of the one-phonon contribution from the raw NIS spectra and the evaluation of the VDOS was carried out using DOS V2.1.[20]

The powder samples were pressed into disk shapes (8 mm diameter), sealed between two beryllium sheets into copper holders with kapton windows and placed nearly horizontally with 5° inclination to the beam, in order to ensure maximum count rate. The liquid samples were prepared ex situ and injected into copper holders coated with parylene-D (so as to avoid corrosion of the copper) and sealed with kapton windows. Measurements were done at around 70 K on three solid reference compounds, $[N(CH_3)_4][FeCl_4]$, $Fe(acac)_3$, and $FeCl_3 \cdot 6H_2O$, and on the frozen solutions of $FeCl_3 \cdot 6H_2O$ dissolved in CPEH both without and with methyl vinyl ketone (MVK) added. Further measurements with enhanced statistics were carried out at around 20 K on $Fe(acac)_3$, on solid $FeCl_3 \cdot 6H_2O$, and on $FeCl_3 \cdot 6H_2O$ dissolved in CPEH.

3. Density Functional Calculations

The geometry optimizations and subsequent frequency calculations in the harmonic approximation were carried out using the BP86 exchange−correlation functional[21,22] and the B3LYP hybrid functional[23,24] as implemented in the Gaussian03 package.[25] For the iron atom, the scalar-relativistic ECP pseudopotential was combined with the corresponding basis set for the Fe valence shells as described in ref 26.

As the usage of different functionals and different basis sets may influence the accuracy of vibrational calculations noticeably, a case study using both pseudopotential and all-electron calculations was carried out for the $FeCl_4^-$ anion. For the Fe atom, an optimized segmented contracted Gauss-type orbital split-valence basis set[27] with contraction scheme {63311/53/41} was used in the all-electron calculations. For the sake of comparison with literature,[28] we also carried out an all-electron calculation where the standard 6-31G* basis set was used for all atoms.

For the carbon, oxygen, chlorine, and hydrogen atoms, Dunning's correlation-consistent double-ζ basis sets[29,30] were used, which were augmented by diffuse functions for the carbon, oxygen, and chlorine atoms in order to take long-range effects into account.

For the calculation of the NIS spectra, use was made of the low-temperature approximation for powder samples[31,32]

$$g(E) = \frac{1}{3}\sum_i e_i^2 = \frac{1}{3}\sum_i \frac{m_{Fe}\langle u_{Fe,i}^2\rangle}{\sum_k m_k\langle u_{k,i}^2\rangle}\delta(E - E_i) \qquad (1)$$

where m_{Fe} is the mass of the resonant Fe atom, $\langle u^2\rangle$ is the mean-square displacement, and i and k are summation indices for the ith mode and the kth atom in this mode, respectively. e_i^2 is also called the mode composition factor.[11,32,33] Finally, the normalization of each vibrational eigenvector with the square root of the reduced mass of the respective mode was taken into account when calculating the vibrational density of states (VDOS).[31] In order to facilitate comparison with experiment, the resulting NIS spectra were convoluted with a Gaussian function possessing the resolution of the NIS experiment.

4. Results and Discussion

Prior to the discussion of the experimental NIS results, we present a case study of theoretically determined vibrational frequencies and bond lengths of the $FeCl_4^-$ anion; see Table 1. In all cases, spin-unrestricted calculations were done on the ground-state sextet.

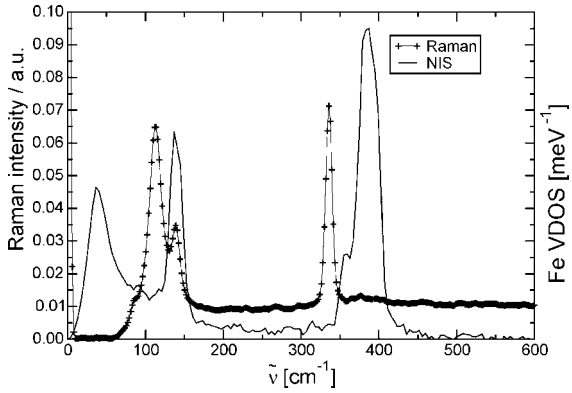

Figure 3. Complementarity of Raman and NIS spectra for solid $[N(CH_3)_4][FeCl_4]$. The Raman data were obtained at room temperature and the NIS data at 70 K.

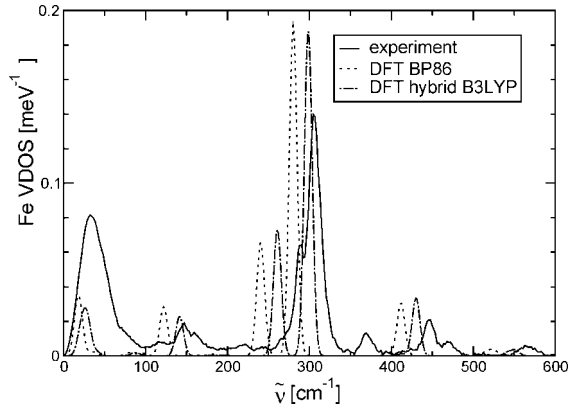

Figure 4. DFT and experimental (T = 20 K) NIS spectra of solid $Fe(acac)_3$.

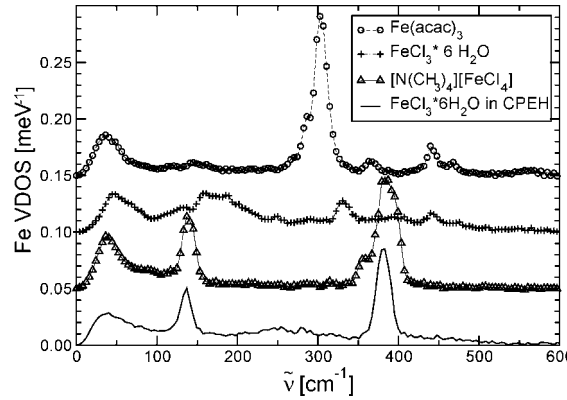

Figure 5. NIS spectrum of three solid reference compounds $Fe(acac)_3$, $FeCl_3 \cdot 6H_2O$, and $[N(CH_3)_4][FeCl_4]$, together with the spectrum of a frozen solution of $FeCl_3 \cdot 6H_2O$ in CPEH at $T = 70$ K. The upper curves are offset for clarity of representation.

Obviously, all theoretical methods give an underestimation of the observed vibrational frequencies, which is, however, less pronounced for the all-electron calculations as compared with that for the pseudopotential method and less pronounced for the B3LYP functional as compared to that for BP86. This can be explained by the fact that with the B3LYP hybrid functional, the exchange energy is treated correctly.

For larger complexes, however, the use of all-electron calculations becomes prohibitively costly in computer time so that in the following, we shall limit ourselves to the pseudopotential methods. A full all-electron Hartree−Fock treatment (see the table) gives a better agreement for some vibrations (not for all) but becomes even more costly for large complexes. Moreover, the bond length is overestimated in the UHF method.

It should be noted that the tetrachloroferrate(III) anion is slightly distorted in the solid,[36] which usually is accompanied by band splitting.[15] In the case of solid $[N(CH_3)_4][FeCl_4]$, the crystallographic asymmetry and hence the distortion of the $FeCl_4^-$ anion by the lattice is relatively small; see also row 1 of Table 1.

The 6-31G* basis set, which has a very moderate quality when compared with the other all-electron basis set, apparently yields the best agreement with experimental wavenumbers. This may, however, be due to error cancelation of limited basis set quality versus the limited quality of the exchange−correlation functional. Thus, we decided to use the more extended basis set as described in section 3 despite the slightly "worse" performance for all further calculations.

Figure 3 shows the complementarity of Raman spectroscopy and NIS at the example of solid tetramethylammonium tetrachloroferrate, thanks to different selection rules. In Raman scattering, the coupling to the radiation field of the incoming and outgoing beam must be taken into account. The dominating modes seen are E, T_2, and A_1 (cf. Table 1). In NIS, the band intensity is simply proportional to the mean-square displacement of the resonant nucleus in the respective mode, leading to exclusive observation of the T_2 modes. Thus, if different isomers of a complex possess different symmetries, this should lead to significant differences in their NIS spectra.

The data for $Fe(acac)_3$, shown in Figure 4, demonstrate again that the faster Becke−Perdew DFT calculations tend to underestimate the experimental wavenumbers by an amount as large as 30 cm^{-1}, whereas the B3LYP method gives much better agreement with experiment. NIS gives access to low-frequency modes, some of which were not visible in a previous FIR study,[35] such as the 28 and 141 cm^{-1} skeletal modes, where the acac units move as a whole with respect to the central Fe atom. Moreover, we wish to emphasize that the DFT calculations were carried out on single molecules and hence neglect intermolecular interactions in the solid.

Figure 5 depicts the vibrational density of states (VDOS) of the iron atoms in four different samples studied by NIS. An additional spectrum (not shown) was measured of the reaction mixture where also the reactant MVK was added. Within the experimental accuracy, this spectrum was identical to the one before the addition of MVK, with however a very slight shift of the 385 cm^{-1} band of $FeCl_4^-$ toward lower frequencies. The absence of $Fe(acac)_3$ or $FeCl_3 \cdot 6H_2O$ and the presence of $FeCl_4^-$ are immediately obvious. The tetrachloroferrate(III) ion was suspected to form as a catalyst poison[4] and shown to be formed together with the bis(ketoester) complex when $FeCl_3 \cdot 6H_2O$ is added to CPEH.[5] We confirm the Raman findings that $FeCl_4^-$ is present, but in addition, we see a number of vibrational bands in the 200−300 cm^{-1} range, which may be compared to the wavenumber (289 cm^{-1}) of the Fe−O stretching vibration in $Fe(acac)_3$.[35]

To improve our findings, the bis(ketoester) complex was measured again with much better statistics and at lower temperature (so as to minimize multiple scattering). The experimental curve, together with the calculated NIS spectrum of $Fe_2Cl_7^-$, is shown in Figure 6. Obviously, the $Fe_2Cl_7^-$ species is not present in the reaction mixture in significant amounts.

The same curve, together with the calculated NIS spectra of the species depicted in Figure 8, is shown in Figure 7.

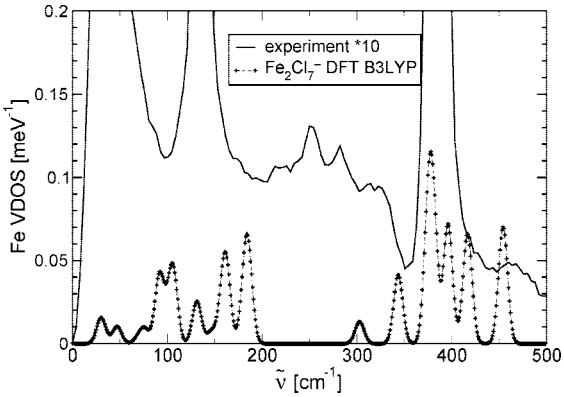

Figure 6. NIS spectrum of a frozen solution of $FeCl_3 \cdot 6H_2O$ in CPEH at $T = 20$ K and the theoretical NIS spectrum of $Fe_2Cl_7^-$ (B3LYP).

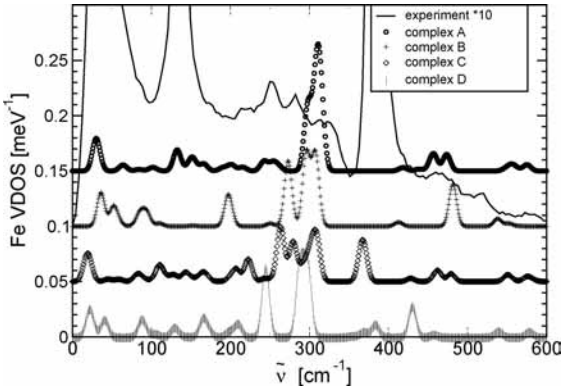

Figure 7. NIS spectrum of frozen reaction mixture of $FeCl_3 \cdot 6H_2O$ in CPEH and DFT B3LYP calculations for the species depicted in Figure 8. The upper curves are offset for clarity of representation.

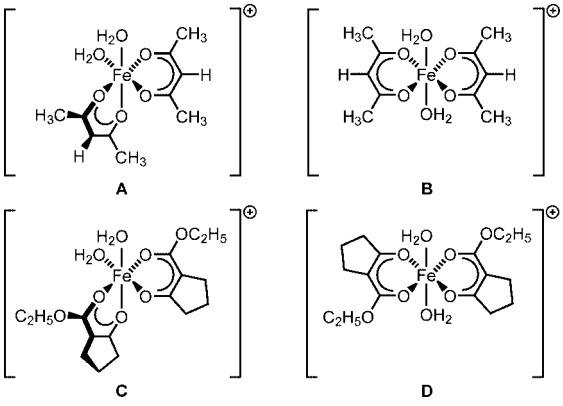

Figure 8. Complexes treated by DFT calculations. The geometries optimized using the BP86 functional are shown; however, the geometries as obtained by B3LYP are almost identical.

It is immediately obvious that the simplified complex (A or B), where $acac^-$ replaces the β-diketo species, gives no good description of the experimental data, that is, that the stiffness introduced by the existence of the cyclopentane ring has a decisive influence on the normal modes around the Fe atom. Moreover, the agreement of the DFT calculation and the experimental data is better for the facial isomer (C) than that for the meridional one (D). Also, for both isomer pairs (A vs B and C vs D), the facial isomers are about $8 \times 10^{-3} E_h$ or 21 kJ mol^{-1} lower in energy than the meridional ones, which is in accord with earlier findings.[4] Thus, we have a strong hint that this species might prevail in solution and maybe also be the complex via which the further reaction proceeds.

5. Conclusions

In the present study, we have demonstrated for the first time that nuclear inelastic scattering on frozen solutions of homogeneous reactions catalyzed by transition-metal complexes is able to reveal the structure of reaction intermediates in homogeneous catalysis. Owing to the special NIS selection rules, isomers that are otherwise very similar may be unambiguously distinguished when experimental statistics are sufficiently good.

Acknowledgment. We wish to thank Prof. Dr. G. Rauhut for support with the Gaussian03 calculations and valuable discussions and Dr. A. I. Chumakov for efficient support at the ID18 beamline. Financial support from the Deutsche Forschungsgemeinschaft within the framework of SFB706 and the Ministerium für Wissenschaft, Forschung und Kunst des Landes Baden-Württemberg, is gratefully acknowledged.

References and Notes

(1) Michael, A. *J. Prakt. Chem.* **1887**, *36*, 113–114.
(2) Christoffers, J. Michael Addition. In *Encyclopedia of Catalysis*; Horvath, I., Ed.;Wiley: New York, 2002; Vol. 5, p 99.
(3) Christoffers, J.; Frey, H. *Chim. Oggi* **2008**, *26*, 26–28.
(4) Pelzer, S.; Kauf, T.; van Wüllen, C.; Christoffers, J. *J. Organomet. Chem.* **2003**, *684*, 308–314.
(5) Bauer, M.; Kauf, T.; Christoffers, J.; Bertagnolli, H. *Phys. Chem. Chem. Phys.* **2005**, *7*, 2664–2670.
(6) Trage, C.; Schröder, D.; Schwarz, H. *Chem.—Eur. J.* **2005**, *11*, 619–627.
(7) Seto, M.; Yoda, Y.; Kikuta, S.; Zhang, X. W.; Ando, M. *Phys. Rev. Lett.* **1995**, *74*, 3828–3831.
(8) Sturhahn, W.; Toellner, T. S.; Alp, E. E.; Zhang, X.; Ando, M.; Yoda, Y.; Kikuta, S.; Seto, M.; Kimball, C. W.; Dabrowski, B. *Phys. Rev. Lett.* **1995**, *74*, 3832–3835.
(9) Chumakov, A. I.; Sturhahn, W. *Hyperfine Interact.* **1999**, *123/124*, 781–808.
(10) Böttger, L. H.; Chumakov, A. I.; Grunert, C. M.; Gütlich, P.; Kusz, J.; Paulsen, H.; Ponkratz, U.; Rusanov, V.; Trautwein, A. X.; Wolny, J. A. *Chem. Phys. Lett.* **2006**, *429*, 189–193.
(11) Sage, J. T.; Paxson, C.; Wyllie, G. R. A.; Sturhahn, W.; Durbin, S. M.; Champion, P. M.; Alp, E. E.; Scheidt, W. R. *J. Phys.: Condens. Matter* **2001**, *13*, 7707–7722.
(12) Achterhold, K.; Parak, F. G. *J. Phys.: Condens. Matter* **2003**, *15*, S1683–S1692.
(13) George, S. J.; Igarashi, R. Y.; Xiao, Y.; Hernandez, J. A.; Demuez, M.; Zhao, D.; Yoda, Y.; Ludden, P. W.; Rubio, L. M.; Cramer, S. P. *J. Am. Chem. Soc.* **2008**, *130*, 5673–5680.
(14) Zeng, W.; Barabanschikov, A.; Zhang, Y.; Zhao, J.; Sturhahn, W.; Alp, E. E.; Sage, J. T. *J. Am. Chem. Soc.* **2008**, *130*, 1816–1817.
(15) Smith, M. C.; Xiao, Y.; Wang, H.; George, S. J.; Coucouvanis, D.; Koutmos, M.; Sturhahn, W.; Alp, E. E.; Zhao, J.; Cramer, S. P. *Inorg. Chem.* **2005**, *44*, 5562–5570.
(16) Petrenko, T.; George, S. D.; Aliaga-Alcalde, N.; Bill, E.; Mienert, B.; Xiao, Y.; Guo, Y.; Sturhahn, W.; Cramer, S. P.; Wieghardt, K.; Neese, F. *J. Am. Chem. Soc.* **2007**, *129*, 11053–11060.
(17) Yabashi, M.; Tamasaku, K.; Kikuta, S.; Ishikawa, T. *Rev. Sci. Instrum.* **2001**, *72*, 4080–4083.
(18) Chang, S.-L.; Stetsko, Yu. P.; Tang, M.-T.; Lee, Y.-R.; Sun, W.-H.; Yabashi, M.; Ishikawa, T. *Phys. Rev. Lett.* **2005**, *94*, 174801.
(19) Chumakov, A. I. Personal communication.
(20) Kohn, V. G.; Chumakov, A. I. *Hyperfine Interact.* **2000**, *125*, 205–221.
(21) Becke, A. D. *Phys Rev. A* **1988**, *38*, 3098–3100.
(22) (a) Perdew, J. P. *Phys Rev. B* **1986**, *33*, 8822–8824. (b) Perdew, J. P. *Phys Rev. B* **1986**, *34*, 7406–7406.
(23) Lee, C.; Yang, W.; Parr, R. G. *Phys. Rev. B* **1988**, *37*, 785–789.
(24) Becke, A. D. *J. Chem. Phys.* **1993**, *98*, 5648–5652.
(25) Frisch, M. J. Trucks, G. W.; Schlegel, H. B.; Scuseria, G. E.; Robb, M. A.; Cheeseman, J. R.; Montgomery, J. A., Jr.; Vreven, T.; Kudin, K. N.; Burant, J. C.; Millam, J. M.; Iyengar, S. S.; Tomasi, J.; Barone, V.; Mennucci, B.; Cossi, M.; Scalmani, G.; Rega, N.; Petersson, G. A.; Nakatsuji, H.; Hada, M.; Ehara, M.; Toyota, K.; Fukuda, R.; Hasegawa, J.; Ishida, M.; Nakajima, T.; Honda, Y.; Kitao, O.; Nakai, H.; Klene, M.; Li, X.; Knox, J. E.; Hratchian, H. P.; Cross, J. B.; Bakken, V.; Adamo, C.; Jaramillo, J.; Gomperts, R.; Stratmann, R. E.; Yazyev, O.; Austin, A. J.; Cammi, R.; Pomelli, C.; Ochterski, J. W.; Ayala, P. Y.; Morokuma, K.; Voth, G. A.; Salvador, P.; Dannenberg, J. J.; Zakrzewski, V. G.; Dapprich, S.; Daniels, A. D.; Strain, M. C.; Farkas, O.; Malick, D. K.; Rabuck, A. D.;

Raghavachari, K.; Foresman, J. B.; Ortiz, J. V.; Cui, Q.; Baboul, A. G.; Clifford, S.; Cioslowski, J.; Stefanov, B. B.; Liu, G.; Liashenko, A.; Piskorz, P.; Komaromi, I.; Martin, R. L.; Fox, D. J.; Keith, T.; Al-Laham, M. A.; Peng, C. Y.; Nanayakkara, A.; Challacombe, M.; Gill, P. M. W.; Johnson, B.; Chen, W.; Wong, M. W.; Gonzalez, C.; Pople, J. A. *Gaussian 03*, revision C.02; Gaussian, Inc.: Wallingford, CT, 2004.

(26) Dolg, M.; Wedig, U.; Stoll, H.; Preuss, H. *J. Chem. Phys.* **1987**, *86*, 866–872.

(27) Schäfer, A.; Horn, H.; Ahlrichs, R. *J. Chem. Phys.* **1992**, *97*, 2571–2577.

(28) Sitze, M. S.; Schreiter, E. R.; Patterson, E. V.; Freeman, R. G. *Inorg. Chem.* **2001**, *40*, 2298–2304.

(29) Dunning, T. H., Jr. *J. Chem. Phys.* **1989**, *90*, 1007–1023.

(30) Kendall, R. A., Jr.; Harrison, R. J. *J. Chem. Phys.* **1992**, *96*, 6796–6806.

(31) Paulsen, H.; Winkler, H.; Trautwein, A. X.; Grünsteudel, H.; Rusanov, V.; Toftlund, H. *Phys. Rev. B* **1999**, *59*, 975–984.

(32) Chumakov, A. I.; Rüffer, R.; Leupold, O.; Sergueev, I. *Struct. Chem.* **2003**, *14*, 109–119.

(33) Sage, J. T.; Durbin, S. M.; Sturhahn, W.; Wharton, D. C.; Champion, P. M.; Hession, P.; Sutter, J.; Alp, E. E. *Phys. Rev. Lett.* **2001**, *86*, 4966–4969.

(34) Avery, J. S.; Burbridge, C. D.; Goodgame, D. M. L. *Spectrochim. Acta* **1968**, *24A*, 1721–1726.

(35) Mikami, M.; Nakagawa, I.; Shimanouchi, T. *Spectrochim. Acta* **1967**, *23A*, 1037–1058.

(36) Wyrzykowski, D.; Kruszýnski, R.; Kłak, J.; Mroziński, J.; Warnke, Z. *Inorg. Chim. Acta* **2008**, *361*, 262–268.

JP806878X